

EBA13²⁰²⁰

13th Brazilian Meeting on Adsorption

DIGITAL

Diana Cristina Silva de Azevedo
Moisés Bastos-Neto
(Organizadores)



UNIVERSIDADE
FEDERAL DO CEARÁ
PRÓ-REITORIA DE
PESQUISA E PÓS-GRADUAÇÃO



FILIADO A



- 057** - Evaluation of LaNiO₃ Type Materials Prepared by Different Routes as Adsorbent for Dyes Removal pp-053
Júlia B. R. Fernandes, Andreza A. Souza, Iasmin A. Ribeiro, Marcelo J. B. Souza, Anne M. Garrido Pedrosa
- 059** - Study of the Influence of Perovskite Structure Site A Metals on the Adsorptive Properties in Liquid Medium pp-059
Jéssica A. S. Lemos, Vitória M. S. C. Souza, Iasmin A. Ribeiro, Marcelo J. B. Souza, Anne M. Garrido Pedrosa
- 065** - Synthesis of LaFeO₃ Material for Application in Congo Red Dye Removal by Adsorption pp-064
Juli E. N. Couto, Iasmin A. Ribeiro, A. M. Garrido Pedrosa, Marcelo. J. B. Souza
- 088** - Synthesis and Characterization of Polyacrylamide-Chitosan Cryogels for Adsorption of Biomolecules pp-070
H. S. D. R. Hamacek, S. M. A. Bueno
- 091** - Diclofenac and Paracetamol Removal from Contaminated Water by Adsorption onto MgAl-Hydroxalcite pp-074
Morgana Rosset, Leticia W. Sfreddo, Oscar W. Perez-Lopez, Liliana Amaral Féris
- 106** - Synthesis and Characterization of Zn–Al–LDH for Application in Adsorption of 2–nitrophenol from Aqueous Solution pp-080
Fabiola Balzan Dalla Nora, Sabrina Frantz Lütke, Lucas Meili, Guilherme Luiz Dotto
- 117** - Synthesis and Characterization of Clay-based Catalysts Prepared from Natural Clays pp-086
A. Santos Silva, Jose L. Diaz de Tuesta, H. T. Gomes, Juliana G. Sgorlon
- 137** - Evaluation of the Influence of H₂S in the Deactivation of Mesoporous Silicas Functionalized with Amino Groups for CO₂ Capture pp-092
Jaryson A. R. de Sousa, Jorge L. B. de Oliveira, Karine O. Moura, Juan A. Cecilia, Enrique Vilarrasa-Garcia, Moisés Bastos-Neto, Diana C.S. de Azevedo
- 142** - Influence of Microwave Radiation on Characteristics of Carbon Composites Based on Resorcinol-Formaldehyde Resin Chars Filled with Carbon Nanotubes pp-098
Mariia Galaburda, Viktor M. Bogatyrov, Anna Deryło-Marczewska, M. Nazarkovsky
- 145** - In situ Synthesis of Zeolite LTA in Glass Fibers Al₂O₃-SiO₂ pp-101
Antonia M. M. França, Marco V. M. do Nascimento, Raquel de A. Bessa, Edipo S. de Oliveira, Adonay R. Loiola, Ronaldo F. do Nascimento
- 178** - Synthesis of a New Adsorbent, from Sugarcane Bagasse, for Removal of As(V) from Aqueous Solution: Using an Agricultural Waste to Water Treatment pp-106
L. C. Maia, M. M. C. E. Carvalho, L. C. Soares, L. V. A. Gurgel

Synthesis and characterization of clay-based catalysts prepared from natural clays

A. Santos Silva^{a,b,c}, Jose L. Diaz de Tuesta^{b,c}, H. T. Gomes^{b,c}, Juliana G. Sgorlon^{a*}

^a Federal University of Technology - Paraná, R. Marçílio Dias, 635 – Jardim Paraíso, Apucarana, 86812600, Brazil

^b Centro de Investigação de Montanha (CIMO), Instituto Politécnico de Bragança, Campus Santa Apolónia, Bragança, 5300252, Portugal

^c Laboratory of Separation and Reaction Engineering-Laboratory of Catalysis and Materials (LSRE-LCM), R. Dr. Roberto Frias, Porto, 4200465, Portugal

Abstract

This work deals with the synthesis and characterization of clay-based catalysts. The catalysts prepared in this work were clays activated through acid treatment and clays pillared with Co and Fe. For the preparation, natural clays from four different regions of Kazakhstan were used: Akzhar, Asa, Karatau and Kokshetau. The FTIR analysis showed that the pillared clays have an amount of iron in its structure. The N₂ adsorption isotherms obtained were classified as Type II, according to IUPAC classification, typical of macroporous materials. The S_{BET} calculated with the N₂ adsorption isotherms for the activated clays showed to be higher than the S_{BET} results for natural clays. XRD patterns helped to gather information about crystalline phases of the clay, allows classifying the type of clay used in the work. The acid characterization showed that the procedures used for the preparation of the acid activated clays and pillared clays caused structural modifications, which is another result that suggests the success of both methods.

Keywords: low-cost materials; pillared clays; activated clays; synthesis and characterization

1. Introduction

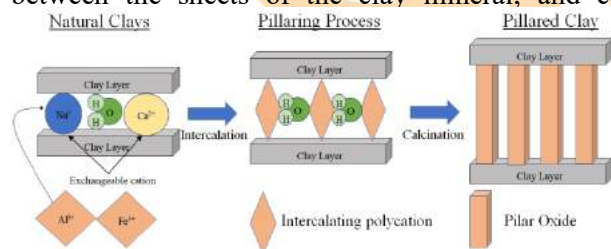
In addition to cost, catalytic properties and availability are important criteria for choosing a good catalyst. This has encouraged the scientific community to search for materials that are both efficient and cheap. There are in the literature several reports of different low-cost materials that can be used as catalysts, such as chitosan hydrogel, lignin and modified clays [1].

Modified clays have been explored for several applications as low-cost materials, showing interesting catalytic and adsorptive properties[2,3]. In the last years, studies about layered aluminosilicate (clays) report its high activity in the Fenton-like process used in the oxidation of organic pollutants. Furthermore, such materials are also a good option for the removal of pollutants by adsorption.

Among modified clays, the pillared clays have been frequently studied for different applications. Pillared clays (PILCs) are porous materials resulting from the process of pillaring lamellar clays. The preparation of pillared clays is one approach to the rational design of porous solids with a pore size

distribution on a molecular length scale. Pillared clays are a special class of intercalated materials in which the intercalant gallery is sufficiently large to allow access to the intracrystal surfaces of the layered structure [4]. Their surface area and permanent porosity allow them to be very attractive solids for adsorption and catalysis purposes.

PILCs can be obtained from smectite clay minerals, which is a phyllosilicate class of minerals with TOT structure, through a procedure that can be divided into three fundamental steps: a) preparation of the pillaring solution that contains the pillaring cations (as for example Al³⁺, Ga³⁺, Ti⁴⁺, Zr⁴⁺, Fe³⁺ and Cr³⁺); b) intercalation of these cations into the interlayer space of the clays, which involves the natural substitution of exchangeable cations present between the sheets of the clay mineral; and c)





during 72 h and then the material was filtered and washed several times until the rinsing waters reach the natural pH. For the last step of the preparation of the pillared clay, the filtered material was dried in an air atmosphere oven at 60 °C overnight and then calcined at 600 °C for 5 h in an air atmosphere muffle. This procedure resulted in the AKP, ASP, KAP and KOP pillared clays from the AKN, ASN, KAN and KON, respectively.

2.2 Characterization

2.2.1 Fourier transformed Infra-red spectroscopy (FTIR)

The FTIR spectra of the 16 different samples were recorded on a Perkin Elmer FT-IR spectrophotometer UATR Two infrared spectrophotometer, with a resolution of 4 cm⁻¹. The range of wavenumber used in the analysis was from 450 to 4000 cm⁻¹. All the measurements were done from the solid samples at room temperature.

2.2.2 Surface and pore analyzer

The textural properties of the materials were determined from N₂ adsorption-desorption isotherms at 77 K, obtained in a Quantachrome instrument NOVA TOUCH LX⁴ using long cells with a bulb and an outer diameter of 9 mm. The specific surface area (S_{BET}) was calculated by the BET method using the software Quantachrome TouchWin, in the range of p/p_0 0.05 – 0.35.

2.2.3 X-ray diffraction (XRD)

The measurements of powder X-ray diffraction (XRD) were obtained by depositing the material in the glass sample holder and analyzing on a diffractometer DRON 3. For the interpretation of the results, the software HighScore Demo was used, from PANalytical.

2.2.4 Acid characterization

One of the tests that can be done for the acid characterization of the clays is the pH of the point of zero charge (pH_{PZC}). For this determination, 0.09 g of clay was added in 6 different erlenmeyers and then 15 mL of 0.01 M NaCl with distinct initial pH values (pH_0) adjusted to different values (2, 4, 6, 8, 10 and 12) by means of 0.02 M NaOH and 0.02 M HCl solutions. The erlenmeyers were placed in an orbital shaker IKA KS 130 Basic and agitated for 24

h at 400 rpm. After the agitation, the suspension was filtered and the pH of the filtrate was measured (pH_F). The pH of the point of zero charge was found in the interception between the curve $pH_0 \times pH_F$ and the identity curve.

The second test used in this work for acid characterization is the acidity and basicity determination. In order to determine the acidity and basicity in the different samples, 0.2 g of catalyst was added in 2 different erlenmeyers. One of the erlenmeyers contained 25 mL of a 0.02 M HCl solution for basicity determination, and the other 25 mL of a 0.02 M NaOH solution for acidity determination. The resulting suspensions in the erlenmeyers were placed in an orbital shaker IKA KS 130 Basic and agitated during 48 h at 400 rpm. After the agitation, the suspension of each erlenmeyer was filtered to remove the solid material, and 20 mL was used for the determination of the concentration by titration. Knowing the concentration of the resulting solution it is possible to obtain the number of moles that react with the acidic or basic centers of the clay, and then, to calculate the acidity and basicity for each sample. Phenolphthalein was used as an indicator in both titrations.

3. Results

3.1. Fourier transformed infra-red spectroscopy (FTIR)

The FTIR spectra obtained by analysis of the different prepared clays are depicted in Fig.3.

In the Kokshetau spectra given in Figure 3(A), it is possible to observe a band appearing at 3,692 cm⁻¹ for the natural clay. This band is due to the –OH stretching vibration for water adsorbed at the interlayer, the reason why this signal is absent in the samples subjected to a calcination treatment [7]. Observing the spectra of Akzhar, Asa, and Karatau clays, it is possible to realize that the natural clays have a band in the range of 1,440 – 1,455 cm⁻¹. This band is due to the presence of calcite in the materials, and its disappearance is a consequence of the exchange between calcium and the pillaring metals, indicating the success of the pillarization [8]. That band was found to be absent in the FTIR spectra of the pillared clays and of the activated clays, explained by the fact that the acid treatment and the pillaring process causes a structural modification.

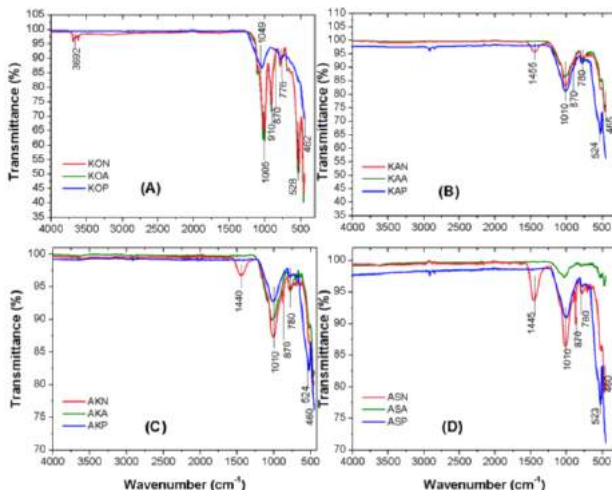


Fig.3. FTIR spectra of the A) Kokshetau clays, B) Karatau clays, C) Akzhar clays and D) Asa clays.

The band in the range of 1,005 to 1,010 cm^{-1} is present in the spectra of all samples and represents the stretching vibrations of the Si–O bond group. The band at 870 cm^{-1} for natural samples can be ascribed to the Al-Mg-OH bending vibrations [7]. The absence of transmittance in this band in the spectra of the pillared samples also could mean that the cation Mg^{2+} was exchanged in the pillaring procedure by the pillaring cations used. In the range of wavenumber from 776 to 780 cm^{-1} , there is a signal of transmittance attributed to the presence of quartz impurity.

The last band, which is present in the range of 460 to 465 cm^{-1} , represents important information deserving special attention. This band is related to the presence of bending vibrations of Si–O–Fe bonds, which is present in all of the samples since the natural clays also contain an amount of these bonds in its structure [9]. The signal of the transmittance in this band is present in AKP, ASP, KAP, and KOP pillared clays, which suggests the successful incorporation of Fe by the pillaring process in the structure of the clay.

3.2. Surface and pore analysis

The adsorption isotherms of N_2 at 77 K on prepared samples are depicted in Fig. 4. As can be observed, the acid activated materials show the highest adsorption capacity. The higher adsorption for the activated sample is less visible for the KOA sample, and this occurs because the acid treatment was not able to significantly increase the surface area of this material. Besides that, the same tendency can be observed in Akzhar, Asa, and Karatau samples, with higher adsorption being

obtained in the activated sample followed by the natural and pillared samples. According to the IUPAC classification, it is possible to conclude that the physisorption isotherms obtained in this work fit in Type II. This classification is attributed to nonporous or macroporous adsorbents, for which the shape of the isotherm is a result of unrestricted monolayer-multilayer adsorption up to high p/p^0 [10].

The results of S_{BET} obtained from the adsorption isotherms are shown in Table 1. The S_{BET} values confirm that the materials with the highest BET surface area are the acid activated clays, which represents a good result since the main goal of this kind of treatment is to increase the surface area of the material. The pillared clays presented a lower surface area than that of the natural clays. This effect occurred by the fact that the calcination treatment done as the last step of the pillaring procedure may have caused the collapse of the pillars. This supposition is valid taking into consideration some works reporting that above 400 °C the pillars collapse in some samples, and this can be the case in this work. Another explanation for the result obtained could be the blockage of the pores of the material with the particles of iron and cobalt, as a consequence of the high concentration of these metals in the pillaring solution.

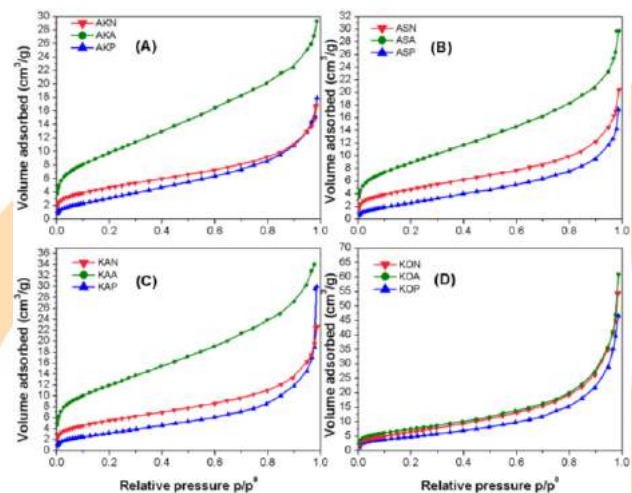


Fig. 4. Adsorption isotherms of N_2 at 77 K of the A) Akzhar clays, B) Asa clays, C) Karatau clays and D) Kokshetau clays.

Table 1- S_{BET} from the materials.

| Material | $S_{\text{BET}}(\text{m}^2/\text{g})$ | Material | $S_{\text{BET}}(\text{m}^2/\text{g})$ |
|----------|---------------------------------------|----------|---------------------------------------|
| AKN | 17 | KAN | 20 |

| | | | |
|-----|----|-----|----|
| AKA | 35 | KAA | 43 |
| AKP | 13 | KAP | 13 |
| ASN | 17 | KON | 26 |
| ASA | 32 | KOA | 28 |
| ASP | 11 | KOP | 19 |

3.3. X- Ray diffraction (XRD)

For this analysis, Karatau and Kokshetau clays were chosen, since they showed the highest surface areas among the clays. Fig. 5 gathers the XRD diffractograms of the analysed samples. Observing the XRD patterns obtained, it is possible to realize that both clays present the typical reflection of montmorillonite [11]. In KAN it is also possible to find traces of saponite, kaolinite, and muscovite [13,14]. In KON, in addition to the already mentioned montmorillonite, there is also the correspondence for the presence of kaolinite [12]. Therefore, both clays can be classified as bentonite, which is the denomination given to the clays composed by a mixture of different clay minerals, with a majority composition of montmorillonite [14].

All the samples present a peak at 26.7° related to the presence of quartz (SiO₂ impurities). The analysis of the diffractograms also allowed the identification of calcite for the Karatau sample and the absence of calcite for Kokshetau samples, which corroborates with FTIR results.

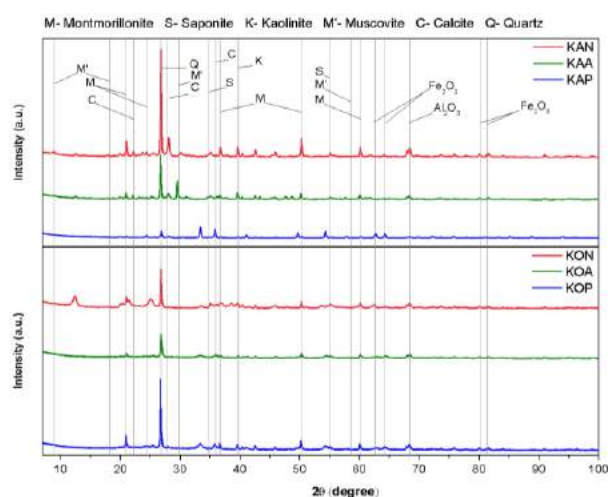


Fig. 5. XRD diffractograms of the A) Karatau samples and B) Kokshetau samples.

It is possible to observe that the signal for SiO₂ and metal oxides such as aluminum oxide and iron oxide [15] decreased in the diffractograms of the

Karatau and Kokshetau samples after the acid treatment. This can be explained by the fact that the acid treatment washed the impurities of SiO₂ from the clay structure, also leaching a small amount of iron metals. For the pillared sample KAP, it is possible to observe that the signal for the SiO₂ impurities decreased and that the signal for the iron oxide increased significantly, putting in evidence the incorporation of iron in the material. In fact, the signal attributed to iron oxide in this sample was higher than in the others.

Finally, in the diffractogram of KOP, the signal for iron oxide was significantly higher than in that observed for the natural sample KON, also confirming the successful incorporation of iron in the clay structure. Besides all the differences between the signals in both diffractograms of the Karatau and Kokshetau samples, it is interesting to observe that the signal for montmorillonite, kaolinite, saponite, and muscovite were not significantly changed in the different samples. This suggests that the structure of the clay is stable, although passing through some structural changes the main structure remained [16].

3.4. X- Acid characterization

The results obtained for both analysis is exposed in Table 2.

Table 2. Results for the acid characterization.

| Samples | Acidity (μmol/g) | Basicity (μmol/g) | pH _{PZC} |
|---------|------------------|-------------------|-------------------|
| AKP | 812 | 538 | 7.15 |
| ASP | 475 | 372 | 7.55 |
| KAP | 687 | 627 | 7.42 |
| KOP | 950 | 652 | 7.37 |
| KOA | 987 | 614 | 7.24 |
| KON | 350 | 245 | 7.77 |

The results obtained for acidity and basicity show that this feature is weak for the samples. As can be observed, all pillared clays have a similar result for the pH_{PZC}, with a difference in the decimal case. An interesting comparison can be done between the samples KOA, KON, and KOP. According to specific studies of pH_{PZC} of pillared clays is expected that the result for the pillared clay is lower than the result obtained with the natural sample. For this work, even than small, it is possible to observe that there is a difference between the pH_{PZC} of the KON and the pH_{PZC} of the KOP, showing that

structural modification has occurred in the clay. Not only the KOP but also the KOA present a different result for pH_{PZC} , which suggests that structural modifications also occurred with the acid treatment [17].

4. Conclusion

The acid activated clays and pillared clays were successfully prepared in this work. The characterization techniques allowed ensuring that structural modification occurred in the clay and that these modifications are related to the formation of the desired materials. In FTIR analysis, for example, the disappearance of the calcite band after the pillaring procedure is the strongest clue of the formation of pillared clays. N_2 adsorption isotherms allowed the calculation of S_{BET} areas, and showed the increase in the area for the acid activated clays, suggesting that the acid activation was successful. XRD analysis reinforced the presence of calcite in natural samples and its absence in pillared samples, which corroborates with FTIR results. At last, the acid characterization results supported the idea that structural modifications occurred in the clay after the acid activation and pillaring procedure.

Acknowledgements

This work is a result of the Project “AIProcMat@N2020 - Advanced Industrial Processes and Materials for a Sustainable Northern Region of Portugal 2020”, with the reference NORTE-01-0145-FEDER-000006, supported by ERDF; the CIMO - UID/AGR/00690/2019 – funded by FCT and FEDER under Programme PT2020 and the Associate Laboratory LSRE-LCM - UID/EQU/50020/2019 - funded by national funds through FCT/MCTES (PIDDAC).

References

- [1] S. T. Khankhasaeva, E. T. Dashinamzhiлова, and D. V. Dambueva, “Oxidative degradation of sulfanilamide catalyzed by Fe/Cu/Al-pillared clays,” *Appl. Clay Sci.*, vol. 146, pp. 92–99, Sep. 2017.
- [2] S. Jain and M. Datta, “Montmorillonite-alginate microspheres as a delivery vehicle for oral extended release of Venlafaxine hydrochloride,” *J. Drug Deliv. Sci. Technol.*, vol. 33, pp. 149–156, 2016.
- [3] W. Yu *et al.*, “Acid-activated and WO_x -loaded montmorillonite catalysts and their catalytic behaviors in glycerol dehydration,” *Chinese J. Catal.*, vol. 38, no. 6, pp. 1087–1100, Jun. 2017.
- [4] H. Shi, T. Lan, and T. J. Pinnavaia, “Interfacial Effects on the Reinforcement Properties of Polymer–Organoclay Nanocomposites,” *Chem. Mater.*, vol. 8, no. 8, pp. 1584–1587, Jan. 1996.
- [5] A. Gil, S. A. Korili, M. A. Vicente, and R. Trujillano, *Pillared Clays and Related Catalysis*. 1994.
- [6] C. N. Rhodes, M. Franks, G. M. B. Parkes, and D. R. Brown, “The effect of acid treatment on the activity of clay supports for $ZnCl_2$ alkylation catalysts,” *J. Chem. Soc. Chem. Commun.*, no. 12, pp. 804–807, 1991.
- [7] T. Li *et al.*, “Design and preparation acid-activated montmorillonite sustained-release drug delivery system for dexibuprofen in vitro and in vivo evaluations,” *Appl. Clay Sci.*, vol. 163, pp. 178–185, Oct. 2018.
- [8] V. J. Bruckman and K. Wriessnig, “Improved soil carbonate determination by FT-IR and X-ray analysis,” *Environ. Chem. Lett.*, vol. 11, no. 1, pp. 65–70, 2013.
- [9] S. Wang, Y. Dong, M. He, L. Chen, and X. Yu, “Characterization of GMZ bentonite and its application in the adsorption of Pb(II) from aqueous solutions,” *Appl. Clay Sci.*, vol. 43, no. 2, pp. 164–171, 2009.
- [10] M. Thommes *et al.*, “Physisorption of gases, with special reference to the evaluation of surface area and pore size distribution (IUPAC Technical Report),” *Pure Appl. Chem.*, vol. 87, no. 9–10, pp. 1051–1069, 2015.
- [11] P. Trigueiro *et al.*, “When anthraquinone dyes meet pillared montmorillonite: Stability or fading upon exposure to light?,” *Dye. Pigment.*, vol. 159, no. June, pp. 384–394, 2018.
- [12] M. Sprynskyy *et al.*, “Preparation of AgNPs/saponite nanocomposites without reduction agents and study of its antibacterial activity,” *Colloids Surfaces B Biointerfaces*, vol. 180, no. April, pp. 457–465, 2019.
- [13] B. L. Zhu *et al.*, “Synthesis, characterization and acid-base properties of kaolinite and metal (Fe, Mn, Co) doped kaolinite,” *Appl. Clay Sci.*, vol. 179, no. April, p. 105138, 2019.
- [14] R. R. Widjaya, A. L. Juwono, and N. Rinaldi, “Bentonite modification with pillarization method using metal stannum,” in *AIP Conference Proceedings*, 2017, pp. 1–7.
- [15] E. Howard and E. Tatge, “Patterns, Chapter 2,” in *Circular of the Bureau of Standards: Standard X-ray diffractions powder patterns*, 1966, pp. 3–84.
- [16] J. Matusik *et al.*, “[Ti,Zr]-pillared montmorillonite – A new quality with respect to Ti- and Zr-pillared clays,” *Microporous Mesoporous Mater.*, vol. 202, pp. 155–164, 2014.
- [17] S. Mnasri, N. Hamdi, N. Frini-Srasra, and E. Srasra, “Acid–base properties of pillared interlayered clays with single and mixed Zr–Al oxide pillars prepared from Tunisian-interstratified illite–smectite,” *Arab. J. Chem.*, vol. 10, no. 8, pp. 1175–1183, 2017.